Reorientable Spin Direction for Spin Current Produced by the Anomalous Hall Effect

Jonathan D. Gibbons,[1] David MacNeill,[1] Robert A. Buhrman,[1] and Daniel C. Ralph[1,2]
[1]*Cornell University, Ithaca, New York 14853, USA*
[2]*Kavli Institute at Cornell for Nanoscale Science, Ithaca, New York 14853, USA*

(Received 12 July 2017; revised manuscript received 20 December 2017; published 20 June 2018)

We show experimentally that the spin direction of the spin current generated by spin-orbit interactions within a ferromagnetic layer can be reoriented by turning the magnetization direction of this layer. We do this by measuring the fieldlike component of spin-orbit torque generated by an exchange-biased $\mathrm{Fe_{95}Gd_5}$ thin film and acting on a nearby $\mathrm{Co_{40}Fe_{40}B_{20}}$ layer. The relative angle of the $\mathrm{Co_{40}Fe_{40}B_{20}}$ and $\mathrm{Fe_{95}Gd_5}$ magnetic moments is varied by applying an external magnetic field. We find that the resulting torque is in good agreement with predictions that the spin current generated by the anomalous Hall effect from the $\mathrm{Fe_{95}Gd_5}$ layer depends on the $\mathrm{Fe_{95}Gd_5}$ magnetization direction $\hat{m}_{\mathrm{FeGd}}$ according to $\vec{\sigma} \propto (\hat{y} \cdot \hat{m}_{\mathrm{FeGd}})\hat{m}_{\mathrm{FeGd}}$, where $\hat{y}$ is the in-plane direction perpendicular to the applied charge current. Because of this angular dependence, the spin-orbit torque arising from the anomalous Hall effect can be nonzero in a sample geometry for which the spin Hall torque generated by nonmagnetic materials is identically zero.

DOI: 10.1103/PhysRevApplied.9.064033

I. INTRODUCTION

Spin-transfer torques exerted by spin currents arising from spin-orbit interactions have the potential to provide greatly improved efficiency in the manipulation of nanomagnetic memory bits. Strong spin-orbit interactions in nonmagnetic heavy metals, for example, can give rise to the spin Hall effect (SHE), which causes electrons with opposite spins to be deflected in opposite transverse directions [1–3]. As a result, when charge current is applied in the plane of a heavy-metal–ferromagnet bilayer the SHE drives injection of spins from the heavy metal into the ferromagnet, generating a spin-transfer torque acting on the magnetization direction, $\hat{m}_{\mathrm{sensor}}$ [4,5]. In typical heavy-metal–ferromagnet bilayers the reflection and rotational symmetries of the sample require that the net orientation $\vec{\sigma}$ of the injected spins is transverse to both the charge current flow and the interface normal. As a consequence, the spin-transfer torque generated by the SHE in such samples is restricted to consist just of an antidamping component that points strictly in plane [of the form $\propto \pm \hat{m}_{\mathrm{sensor}} \times (\vec{\sigma} \times \hat{m}_{\mathrm{sensor}})$] plus a fieldlike torque (of the form $\propto \pm \vec{\sigma} \times \hat{m}_{\mathrm{sensor}}$) [6,7]. This restriction can be detrimental for applications; an antidamping torque that lies in the sample plane is incapable of driving highly efficient antidamping switching of devices with perpendicular magnetic anisotropy [8]. The symmetry requirement that mandates the fixed direction of $\vec{\sigma}$ can be relaxed by using single-crystal spin-orbit materials with sufficiently low crystal symmetries [7], but it will be difficult to incorporate such materials into practical technologies.

Electrons inside ferromagnetic metals, like those in nonmagnetic heavy metals, can also undergo spin-dependent deflection. This deflection produces the well-known anomalous Hall effect (AHE) [9], and is also expected to create charge-current—spin-current interconversion in ferromagnets analogous to the SHE and inverse spin Hall effect (ISHE) in nonmagnetic metals. In fact, the ISHE has already been observed in a variety of ferromagnetic materials [10–15], and spin accumulations due to the anomalous Hall effect have also been reported [16,17]. However, the transverse spin currents arising from spin-orbit interactions within a ferromagnet are predicted to have a qualitatively different character than the SHE in a nonmagnetic heavy metal due to the presence of the strong ferromagnetic exchange field [18,19]. Spins in a ferromagnet precess rapidly around the magnetization (exchange-field) direction, so that any net macroscopic spin current within a ferromagnetic layer should have the spin polarized along $\pm\hat{m}_{\mathrm{source}}$, where $\hat{m}_{\mathrm{source}}$ is the magnetic-moment orientation of the source layer. This suggests that it should be possible to reorient the polarization of the spin current produced by spin-orbit interactions within a ferromagnet by reorienting $\hat{m}_{\mathrm{source}}$, to thereby gain the ability to reorient at will both the antidamping torque and the fieldlike torque that the spin current applies to a second magnetic layer. Here, we report measurements of a spin-orbit-induced spin current generated from a source magnetic layer, detected by measuring the fieldlike spin-transfer torque applied to a second, spin-absorbing sensor magnetic layer [Fig. 1(a)]. We observe the predicted [18,19] reorientation of the injected spins as the source-layer moment is rotated in the sample plane. As one consequence, we show that the spin current generated by a ferromagnetic source layer is able to apply spin-transfer torque in a sample configuration where the conventional spin Hall torque produced by a nonmagnetic heavy metal is zero.

II. MATERIALS AND CHARACTERIZATION

For our experiments, we use a thin-film stack comprising a 10-nm $\mathrm{IrMn_3}$ layer, followed by a 4 nm $\mathrm{Fe_{95}Gd_5}$ source layer, a 2-nm Hf spacer [20], and a 2-nm $\mathrm{Co_{40}Fe_{40}B_{20}}$ sensor layer capped with 3 nm of Hf. Our films are grown on sapphire wafers via dc magnetron sputtering, annealed at 420 K for one hour in a 0.2-T in-plane magnetic field to set the exchange bias direction of the $\mathrm{IrMn_3}$ layer, and then patterned into 120-μm by 20-μm Hall bars with 5-μm voltage probes using optical lithography and ion milling, with the current direction aligned approximately with the exchange bias direction [Fig. 1(a)]. We choose $\mathrm{Fe_{95}Gd_5}$ as our spin-source material because rare-earth ferromagnetic alloys have the potential for efficient spin-current generation—in particular, past research [28] has found that certain iron-gadolinium alloys may exhibit a strong anomalous Hall effect. (We have not yet attempted optimization of the Gd concentration.) The exchange bias from $\mathrm{IrMn_3}$ acting on the $\mathrm{Fe_{95}Gd_5}$ layer allows us to control the angle between the magnetic moments of the $\mathrm{Co_{40}Fe_{40}B_{20}}$ and $\mathrm{Fe_{95}Gd_5}$ layers, and therefore to study whether the orientation $\vec{\sigma}$ of the spin current produced by current flow in the $\mathrm{Fe_{95}Gd_5}$ layer depends on the $\mathrm{Fe_{95}Gd_5}$ moment orientation. To obtain the most accurate control over this offset angle, the samples are designed to have in-plane magnetic anisotropy and our external magnetic fields are also applied in plane; the soft $\mathrm{Co_{40}Fe_{40}B_{20}}$ layer saturates along even weak external fields, whereas the $\mathrm{Fe_{95}Gd_5}$ layer rotates smoothly from the exchange bias direction to the applied field direction as the strength of the external field is increased. The exchange bias grows with decreasing temperatures, so we perform all measurements at cryogenic temperatures, approximately 30 K. The 30-K resistivities of the various layers, determined by measurements of separate test samples, are approximately $209 \pm 20\ \mu\Omega\,\mathrm{cm}$ ($\mathrm{IrMn_3}$), $64 \pm 8\ \mu\Omega\,\mathrm{cm}$ ($\mathrm{Fe_{95}Gd_5}$), $80 \pm 20\ \mu\Omega\,\mathrm{cm}$ (Hf), and $94 \pm 35\ \mu\Omega\,\mathrm{cm}$ ($\mathrm{Co_{40}Fe_{40}B_{20}}$).

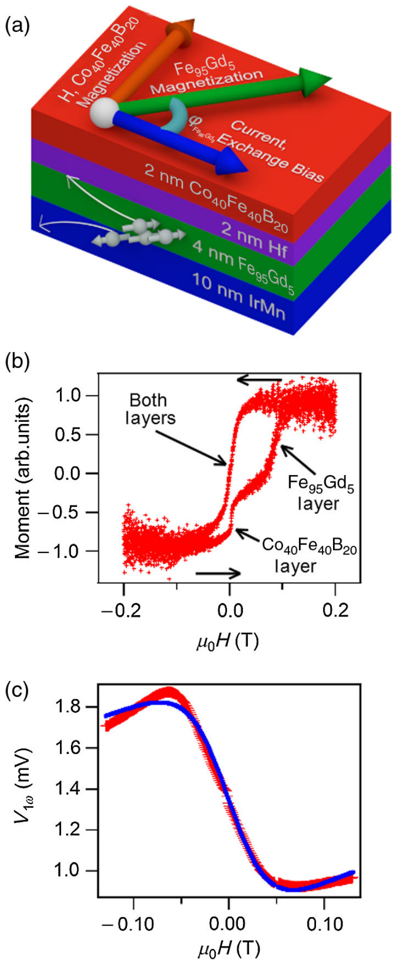

FIG. 1. (a) Schematic of the device geometry. (b) Magnetization of an unpatterned $\mathrm{IrMn_3/Fe_{95}Gd_5/Hf/Co_{40}Fe_{40}B_{20}/Hf}$ multilayer at 30 K measured using vibrating sample magnetometry, showing the exchange-biased switching of the $\mathrm{Fe_{95}Gd_5}$ layer with high coercivity, and the low-coercivity switching of the $\mathrm{Co_{40}Fe_{40}B_{20}}$ layer. (c) First harmonic Hall data (red markers) taken at 30 K, with the exchange bias parallel to the current and the magnetic field perpendicular to the exchange bias. The value of the $\mathrm{Fe_{95}Gd_5}$ layer exchange bias is extracted from the fit (blue line) to the planar Hall signal.

Figure 1(b) shows a measurement of the magnetization of our unpatterned film stack as a function of a magnetic field applied in the sample plane parallel to the set exchange bias, as characterized by vibrating sample magnetometry (VSM) at 30 K. When increasing the magnetic field from zero, we see first the in-plane magnetization switching of the low-coercivity $\mathrm{Co_{40}Fe_{40}B_{20}}$ sensor layer. This is followed at higher fields by the more gradual switching of the strongly exchange-biased $\mathrm{Fe_{95}Gd_5}$ layer. These data verify that both magnetic layers have in-plane magnetic anisotropy.

III. SECOND-HARMONIC HALL METHOD FOR MAGNETIC SPIN HALL LAYERS

To measure current-induced torques on the sensor layer (which can arise from either spin currents or an Oersted field) we use the second-harmonic Hall technique [6,29–32] in which a low-frequency (1000 Hz) alternating current is applied to the device and the induced Hall voltage is measured at the second-harmonic frequency. For all samples, we apply a 5-V signal, so that the current density within a given material layer is approximately the same between samples. In principle, for an in-plane-magnetized sample the second-harmonic Hall technique can provide measurements of both the in-plane and out-of-plane components of current-induced torque, and can also distinguish antidamping torques from fieldlike torques (see Fig. 2), but one must be careful to distinguish the spin-torque signals from artifacts associated with thermoelectric effects [31]. In-plane torques correspond to out-of-plane effective magnetic fields (by the right-hand rule) so that they tend to pull an in-plane sensor layer slightly out of plane, giving a second-harmonic Hall voltage signal on account of mixing between an oscillating anomalous Hall resistance and the

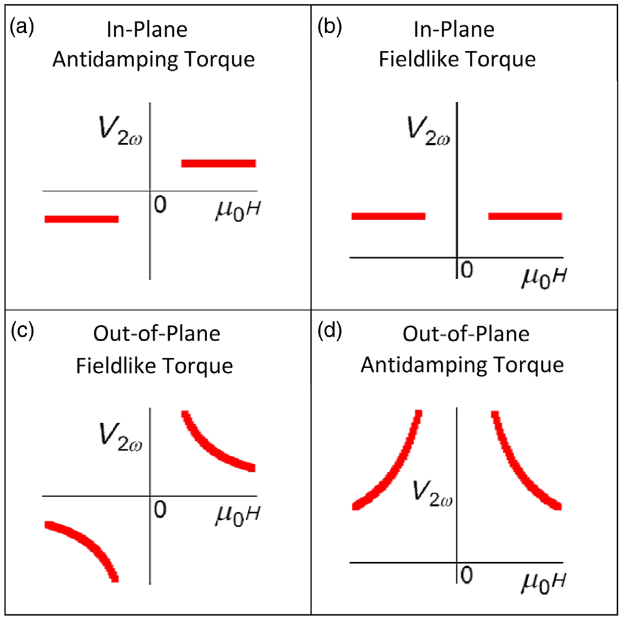

FIG. 2. Predicted second-harmonic Hall signals resulting from various forms of spin torque acting on a ferromagnetic sensor layer with in-plane magnetization for applied fields near zero. These results assume that the spin torque is nonzero and does not vary strongly with the applied magnetic field near $H = 0$.

oscillating current. In this case, the in-plane torque competes with both the magnetic anisotropy field H_k of the thin-film $Co_{40}Fe_{40}B_{20}$ layer and the applied magnetic field H, to give a second-harmonic signal amplitude $\propto 1/(H_k + |H|)$, and because $H_k \gg |H|$ in our experiment, the magnitude of the second-harmonic Hall signal should be small and approximately independent of the magnitude of the applied magnetic field for a fixed field orientation near $H = 0$. For the usual case of an antidamping in-plane torque, flipping the magnetization direction of the sensor layer changes the sign of the deflection, so that the final second-harmonic Hall signal should have a sign change near $H = 0$ upon reversal of our low-coercivity $Co_{40}Fe_{40}B_{20}$ layer, and should otherwise be flat as a function of swept magnetic field [Fig. 2(a)]. [In the presence of a fieldlike in-plane torque, reversing the sensor layer would not change the sign of the second-harmonic signal, Fig. 2(b).] Out-of-plane torques, on the other hand, correspond to in-plane effective fields, causing an in-plane rotation of the sensor layer's magnetization that is detected through mixing with the planar Hall resistance. This in-plane field competes only with the applied magnetic field. The size of the sensor layer deflection is then inversely proportional to the applied field, and we expect a second-harmonic Hall signal whose magnitude diverges as $1/|H|$. For a fieldlike out-of-plane torque, reversing the $Co_{40}Fe_{40}B_{20}$ magnetization direction changes the sign of the second-harmonic signal, so that the signal should flip sign as the field is swept through zero to reorient the low-coercivity $Co_{40}Fe_{40}B_{20}$ layer [Fig. 2(c)], while for an antidamping out-of-plane torque the signal would be proportional to $1/|H|$ with no sign change [Fig. 2(d)]. All of the entries in Fig. 2 assume that the spin-current-induced torque is nonzero and approximately independent of magnetic field in the range near $H = 0$; if the magnitude of the torque depends on field there will be deviations (as discussed below) from the ordinary $1/|H|$ dependence for out-of-plane torques and H-independent behavior for in-plane torques.

To best distinguish whether there is a spin-orbit torque arising from the magnetic $Fe_{95}Gd_5$ layer that depends on the orientation of the $Fe_{95}Gd_5$ moment, we consider a measurement configuration for which the torques arising from both the current-generated Oersted field and also any conventional spin Hall effect must be zero. We sweep the applied magnetic field perpendicular to the current flow direction (and therefore also perpendicular to the direction of the exchange bias), so that the low-coercivity $Co_{40}Fe_{40}B_{20}$ sensor layer is quickly saturated perpendicular to the current (for $|\mu_0 H|$ greater than approximately 0.01 Tesla), while the angle φ_{FeGd} of the $Fe_{95}Gd_5$ moment rotates slowly away from the exchange bias direction with increasing field magnitude [see Fig. 1(a)]. Fitting to the planar Hall first harmonic data [Fig. 1(c)] allows us to extract the value of the exchange bias field as $\mu_0 H_{\mathrm{ex}} = 0.070 \pm 0.001$ T. Because the sensor-layer moment is oriented transverse to the current flow direction (i.e., along the Oersted field), there can be no Oersted torque on the sensor layer. Likewise, in this geometry the sensor moment is also parallel to the spins that would be created by any conventional spin Hall effect, so that there can be no conventional spin Hall torque. This geometry has the further advantage that any possible artifacts from the anomalous Nernst effect or the longitudinal spin Seebeck effect in the $Co_{40}Fe_{40}B_{20}$ layer must also be zero (since for either mechanism $V_{\mathrm{Hall}} \propto \mathbf{\nabla} T \times \hat{m}$, and the thermal gradient $\mathbf{\nabla} T$ is assumed to be out of plane [31,33–35]).

IV. RESULTS

Our experimental results in this geometry for the second-harmonic Hall voltage as a function of the applied magnetic field (perpendicular to the applied charge current direction) are shown in Fig. 3(a). We have excluded data for field magnitudes less than 0.01 T from our analysis, because in this regime the $Co_{40}Fe_{40}B_{20}$ layer undergoes a spatially nonuniform reversal process that invalidates the macrospin assumption we use to interpret the second-harmonic Hall measurements. An artifact due to coupling between the magnetic layers can also exist in this very low field range (see Supplemental Material [36]). We will exclude the same range of field for all data analyzed below from samples containing the $Co_{40}Fe_{40}B_{20}$ layer. We observe in Fig. 3(a) a substantial signal whose magnitude diverges approximately as $1/|H|$ as H approaches zero, with a sign change as H is swept through 0. This is the signature of an out-of-plane fieldlike torque [Fig. 2(c)]. Because the low-coercivity $Co_{40}Fe_{40}B_{20}$ sensor is the only layer that reverses near

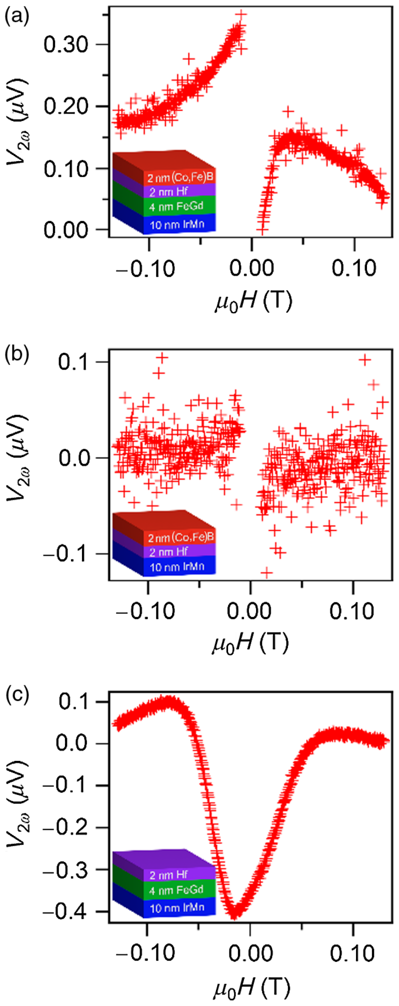

FIG. 3. (a) The measured second-harmonic Hall signal at 30 K for the full $IrMn_3/Fe_{95}Gd_5/Hf/Co_{40}Fe_{40}B_{20}/Hf$ multilayer with the exchange bias approximately parallel to the current and the magnetic field applied in plane and perpendicular to the current. (b),(c) The second-harmonic Hall signals measured under the same conditions for (b) the $IrMn_3/Hf/Co_{40}Fe_{40}B_{20}/Hf$ control sample and (c) the $IrMn_3/Fe_{95}Gd_5/Hf$ control sample. Field-independent backgrounds have been subtracted from each data set.

$H = 0$ (while the $Fe_{95}Gd_5$ magnetization remains oriented near the exchange bias direction), this behavior indicates that the signal arises from a torque on the $Co_{40}Fe_{40}B_{20}$ sensor layer. Unlike the schematic curve sketched in Fig. 2(c), the magnitude of this spin-current-induced torque is not constant, but rather changes as a function of changing field magnitude, and hence as a function of changing φ_{FeGd}. This is evident because if the magnitude of the torque were constant, the magnitude of the second-Harmonic Hall signal should decrease monotonically with increasing field magnitude as $\propto 1/|H|$, while the data display a distinctly nonmonotonic dependence at positive field, with $V_{2\omega}$ initially increasing and then decreasing as $\mu_0 H$ increases from 0.

To rule out potential experimental artifacts, we prepare two control samples: (i) $IrMn_3$(10 nm)/Hf(2 nm)/$Co_{40}Fe_{40}B_{20}$(2 nm)/Hf(3 nm) and (ii) $IrMn_3$(10 nm)/$Fe_{95}Gd_5$(4 nm)/Hf(3 nm), the first having no $Fe_{95}Gd_5$ layer, and the second having no $Co_{40}Fe_{40}B_{20}$ layer. We perform the same second-harmonic Hall measurement on each of these samples, with the applied magnetic field perpendicular to the current direction. The sample with no $Fe_{95}Gd_5$ layer exhibits no field-dependent signal [Fig. 3(b)]. This is as expected, because (as noted above) the orientation of the $Co_{40}Fe_{40}B_{20}$ moment transverse to the current should prevent any signals due to spin Hall or Oersted torques and also any thermal signals due to the Nernst effect. Both of these mechanisms should depend only on the behavior of the $Co_{40}Fe_{40}B_{20}$ layer; therefore, this measurement allows us to confirm that these signals are indeed absent in our geometry.

The control sample containing only the exchange-biased $Fe_{95}Gd_5$ layer shows a signal consistent with a dominant contribution from an out-of-plane Oersted torque acting on the $Fe_{95}Gd_5$ layer and contributing to the Hall voltage via a planar Hall effect, with a small angular misalignment of the exchange bias direction [Fig. 3(c)] (this signal is nonzero because the exchange-biased $Fe_{95}Gd_5$ moment is not oriented transverse to the current). The control sample also shows a small signal due to the anomalous Nernst effect (see Supplemental Material [36]). The signal consists of a dip with maximum amplitude centered near $H = 0$ where the $Fe_{95}Gd_5$ moment is parallel to the current, so that the Oersted torque on the $Fe_{95}Gd_5$ moment is maximal. The result is, therefore, qualitatively different from the divergences with a sign change in Fig. 3(a). The Oersted torque should be substantially smaller in our full stack than in the $Fe_{95}Gd_5$ control sample, because in the full stack the part of the Oersted field acting on the $Fe_{95}Gd_5$ layer that is generated in the Hf and $Co_{40}Fe_{40}B_{20}$ layers partially cancels the part of the Oersted field generated in the $IrMn_3$ layer. We can estimate the size of this signal in our full stack (see Supplemental Material [36]) from the control measurements, and include this signal as a background in our analysis as described below.

Based on the data in Fig. 3(a) and from the two control samples [Figs. 3(b) and 3(c)] we conclude that the out-of-plane fieldlike torque signal observed near $H = 0$ in Fig. 3(a) is due to a spin current arising from the $Fe_{95}Gd_5$ layer and acting on the $Co_{40}Fe_{40}B_{20}$ layer. This cannot be a conventional spin-orbit torque due to the spin Hall effect, because the conventional spin-transfer torque is zero for a magnetic sensor layer oriented perpendicular to the current flow.

V. SECOND-HARMONIC HALL MODEL FOR REORIENTABLE SPIN CURRENT

To analyze more quantitatively the spin-transfer torque exerted by the $Fe_{95}Gd_5$ layer acting on the $Co_{40}Fe_{40}B_{20}$

layer, we compare to the theory of Taniguchi *et al.* [19], in which spin-orbit coupling within the ferromagnetic source layer ($\mathrm{Fe_{95}Gd_5}$) generates a transverse spin current with polarization

$$\vec{\sigma} \propto (\hat{y} \cdot \hat{m}_{\mathrm{FeGd}})\hat{m}_{\mathrm{FeGd}}, \tag{1}$$

where $\hat{m}_{\mathrm{FeGd}}$ is a unit vector along the $\mathrm{Fe_{95}Gd_5}$ magnetization direction, and $\hat{y}$ is the in-plane direction perpendicular to the applied charge current. Intuitively, we can think of this as a projection of the ordinary SHE spin current onto the magnetization direction [37]. Because our system uses an in-plane ferromagnetic sensor layer, it is more sensitive to out-of-plane torques than in-plane torques. If the spin polarization from the source layer interacts with the sensor layer through an effective field $\propto\vec{\sigma}$ [producing an out-of-plane fieldlike (FL) torque], then the effective field produced is $\vec{H}_{\mathrm{FL}} = \hat{m}_{\mathrm{FeGd}} H^0_{\mathrm{FL}} \sin(\varphi_{\mathrm{FeGd}})$. The expected second-harmonic signal (V_H^{2f}) for the case that the external field H is swept perpendicular to the current-flow direction is (see Supplemental Material [36])

$$V_H^{2f} = -IR_{\mathrm{PHE}} \cos(2\varphi_{\mathrm{CoFeB}}) \times \frac{H^0_{\mathrm{FL}} \sin(\varphi_{\mathrm{FeGd}}) \sin(\varphi_{\mathrm{CoFeB}} - \varphi_{\mathrm{FeGd}})}{2|H|}. \tag{2}$$

Here, I is the applied current, R_{PHE} is the planar Hall coefficient of the multilayer due to the $\mathrm{Co_{40}Fe_{40}B_{20}}$, and φ_{CoFeB} is the angle between the current and the magnetic field, which is either 90° or −90°, following the sign of the applied magnetic field. The H dependence of V_H^{2f} comes from the H dependence of φ_{FeGd} and the susceptibility term $1/|H|$. To model the data in Fig. 3(a), it is essential to take into account that the direction of the exchange bias on the $\mathrm{Fe_{95}Gd_5}$ layer ($\varphi^0_{\mathrm{FeGd}}$) is slightly misaligned from the current direction, so that $\varphi_{\mathrm{FeGd}} \approx \varphi^0_{\mathrm{FeGd}} + \tan^{-1}(H/H_{\mathrm{ex}})$. If $\varphi^0_{\mathrm{FeGd}}$ were exactly zero, the spin torque would go to zero for $H = 0$, so that the divergent part of the signal in Fig. 3(a) would not be present. Furthermore, the fact that φ_{FeGd} sweeps through zero at a nonzero value of the H contributes to the asymmetry in Fig. 3(a) away from $H = 0$. Our fits suggest a misalignment $\varphi^0_{\mathrm{FeGd}} \approx 3.1°$. Figure 4(b) shows the dependence of φ_{FeGd} on the magnetic field based on the fitted values of $\varphi^0_{\mathrm{FeGd}}$ and H_{ex}, and Fig. 4(c) shows the corresponding changes in φ_{CoFeB}.

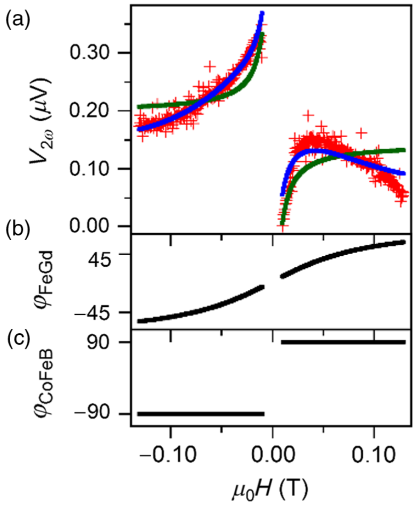

FIG. 4. (a) The same data (red markers) as in Fig. 3(a), with comparison to the model of Taniguchi *et al.* [19] (blue line), which assumes that $\vec{\sigma} \propto (\hat{y} \cdot \hat{m}_{\mathrm{FeGd}})\hat{m}_{\mathrm{FeGd}}$, as well as a fit to a model which assumes that $\vec{\sigma}$ is constant (green line). (b), (c) Dependence on the applied magnetic field for the magnetization angles φ_{FeGd} and φ_{CoFeB} within the fit.

VI. DISCUSSION

In performing our fits, we can also account for a small contribution due to the Oersted torque on the $\mathrm{Fe_{95}Gd_5}$ layer, detected in the Hall voltage via the $\mathrm{Fe_{95}Gd_5}$ planar Hall effect. We estimate the size of this background signal generated by the Oersted torque independently (see Supplemental Material [36]). Furthermore, we account for a Nernst signal generated in the $\mathrm{Co_{40}Fe_{40}B_{20}}$ due to angular misalignment of the sample with respect to the applied field. All of these effects are small; a full discussion (and our procedures for accounting for them) is included in the Supplemental Material [36].

Figure 4(a) shows the same second-harmonic Hall data as in Fig. 3(a) with a fit to the theory of Taniguchi *et al.* [19] (blue line) (see Supplemental Material [36]). The fit conforms well to the measured data. Unlike the schematic in Fig. 2(c), the second-harmonic signal does not decrease symmetrically to zero at large positive and negative fields. This is because the spin torque is not constant as a function of changing H, but changes as H reorients φ_{FeGd}. To illustrate the necessity of taking into account the variation of the transverse spin current $\vec{\sigma}$ on the orientation of the $\mathrm{Fe_{95}Gd_5}$ moment [Eq. (1)], we have also performed a fit corresponding to the assumptions of Fig. 2(c), that $\vec{\sigma}$ is a constant, independent of φ_{FeGd} (green line). [This is somewhat artificial, since for the experimental geometry of Fig. 3(a) one should have $\vec{\sigma} = 0$ for conventional torques, as explained above.] Any model assuming $\vec{\sigma} = $ constant is qualitatively inconsistent with the measurements, while taking into account the expected variation of $\vec{\sigma}$ with φ_{FeGd} accounts well for the nonmonotonic dependence of the signal at positive fields.

We can characterize the strength of the out-of-plane fieldlike torque generated by the $\mathrm{Fe_{95}Gd_5}$ and acting on the $\mathrm{Co_{40}Fe_{40}B_{20}}$ in terms of a spin-torque efficiency $\xi_{\mathrm{FL,AHE}}$, such that the spin-current-induced effective field acting on the $\mathrm{Co_{40}Fe_{40}B_{20}}$ is $H^0_{\mathrm{FL}} = \xi_{\mathrm{FL,AHE}}(\hbar/2e\mu_0 M_s t_{\mathrm{FM}}) \times J_e \sin(\varphi_{\mathrm{FeGd}})$, where J_e is the applied charge current density in the $\mathrm{Fe_{95}Gd_5}$, $\mu_0 M_s = 0.90$ T is the saturation magnetization of the $\mathrm{Co_{40}Fe_{40}B_{20}}$ layer based on VSM measurements of a $\mathrm{IrMn_3/Hf/Co_{40}Fe_{40}B_{20}/Hf}$ control sample, and t_{FM} is the thickness of the ferromagnetic layer. Fitting the measured signal yields an estimated $\xi_{\mathrm{FL,AHE}}$ of $-0.9 \pm 0.2\%$. This value is a lower bound for the magnitude of the fieldlike spin-torque efficiency that can be generated by the $\mathrm{Fe_{95}Gd_5}$ because we do not account for less-than-perfect interface transparency or the loss of spin current upon transmission through the hafnium, which has a spin diffusion length of approximately 1.5 nm [21]. An in-plane torque component may also be present in our samples, but the experimental geometry does not allow an accurate quantitative measurement. The signature of an in-plane torque in a second-harmonic Hall measurement is much less pronounced than the $1/|H|$ divergence for an out-of-plane torque, and is further obscured when the magnitude of the torque is field dependent. Our best estimate, based on multiparameter fits, is that the analogous antidamping torque efficiency is $|\xi_{\mathrm{AD,AHE}}| < 1.0\%$ (see Supplemental Material [36]). That the dampinglike torque is not much stronger than the fieldlike torque may be a consequence of the $\mathrm{Hf/Co_{40}Fe_{40}B_{20}}$ interface. Previously, we have observed that even though $\xi_{\mathrm{AD}} \gg \xi_{\mathrm{FL}}$ in $\mathrm{W/Fe_{60}Co_{20}B_{20}}$ devices that after the addition of a Hf spacer $\xi_{\mathrm{AD}} < \xi_{\mathrm{FL}}$ in $\mathrm{W/Hf/Fe_{60}Co_{20}B_{20}}$ [21].

We note that Humphries *et al.* [38] have recently pointed out an alternative mechanism whereby an out-of-plane spin-orbit torque might be generated in a ferromagnet-spacer-ferromagnet multilayer—a spin current generated by spin-orbit interactions with an in-plane spin polarization might precess in the exchange field of the fixed magnetic layer so that when the resulting spin current interacts with the sensor magnetic layer it can apply an out-of-plane antidamping torque. We can tell that this mechanism is not dominant in our measurement because the out-of-plane torque we measure is a fieldlike torque, not an antidamping torque, based on the sign change we observe in the component of the second-harmonic Hall signal proportional to $1/|H|$ upon reversal of the $\mathrm{Co_{40}Fe_{40}B_{20}}$ magnetization near zero field.

VII. CONCLUSIONS

In summary, we observe experimentally an out-of-plane fieldlike spin-orbit torque that varies in strength as a function of changes in the direction of the magnetic moment in the source layer. These changes are quantitatively consistent with predictions [18,19] for the variations in the spin current resulting from the anomalous Hall effect within the magnetic layer. The most direct evidence for spin torque from this mechanism is that it can deflect sensor-layer magnetic moments oriented perpendicular to the charge current flow, whereas both conventional spin Hall torques and the current-induced torque from the Oersted field are identically zero for this geometry. The results we report have been obtained using magnetic layers with in-plane magnetic anisotropy, in order to obtain the best control over magnetic orientations and the fewest competing experimental artifacts, which has the consequence that these measurements are primarily sensitive to an out-of-plane fieldlike component of spin-orbit torque. We have not yet probed the regime of our primary interest for practical applications—in which $\hat{m}_{\mathrm{source}}$ is tilted out of the sample plane so that the anomalous Hall effect mechanism might apply an antidamping torque to an active magnetic layer with perpendicular magnetic anisotropy. However, the good agreement between theory [19] and our results with in-plane magnetized layers provides optimism for the pursuit of this goal.

Machine-readable access to all data is available at [40].

ACKNOWLEDGMENTS

We thank G. Stiehl for comments on the manuscript. This work was supported by the National Science Foundation (No. DMR-1406333, No. DMR-1708499) and Western Digital. We made use of the Cornell Nanoscale Facility, a member of the National Nanotechnology Coordinated Infrastructure (NNCI), which is supported by the NSF (ECCS-1542081), and also the Cornell Center for Materials Research Shared Facilities, which are supported by the NSF MRSEC program (DMR-1719875).

Note added.—Recently, we became aware of Bose *et al.*'s paper [39] on related work with different conclusions.

[1] M. I. D'yakonov and V. I. Perel, Possibility of orienting electron spins with current, JETP Lett. **13**, 467 (1971) [http://www.jetpletters.ac.ru/ps/1587/article_24366.shtml].

[2] J. E. Hirsch, Spin Hall Effect, Phys. Rev. Lett. **83**, 1834 (1999).

[3] S. Zhang, Spin Hall Effect in the Presence of Spin Diffusion, Phys. Rev. Lett. **85**, 393 (2000).

[4] I. M. Miron, K. Garello, G. Gaudin, P.-J. Zermatten, M. V. Costache, S. Auffret, S. Bandiera, B. Rodmacq, A. Schuhl, and P. Gambardella, Perpendicular switching of a single ferromagnetic layer induced by in-plane current injection, Nature (London) **476**, 189 (2011).

[5] Luqiao Liu, Chi-Feng Pai, Y. Li, H. W. Tseng, D. C. Ralph, and R. A. Buhrman, Spin torque switching with the giant spin Hall effect of tantalum, Science **336**, 555 (2012).

[6] K. Garello, I. M. Miron, C. O. Avci, F. Freimuth, Y. Mokrousov, S. Blugel, S. Auffret, O. Boulle, G. Gaudin, and P. Gambardella, Symmetry and magnitude of spin-orbit torques in ferromagnetic heterostructures, Nat. Nanotechnol. **8**, 587 (2013).

[7] D. MacNeill, G. M. Stiehl, M. H. D. Guimaraes, R. A. Buhrman, J. Park, and D. C. Ralph, Control of S-O torques through crystal symmetry in $\mathrm{WTe_2}$/ferromagnet bilayers, Nat. Phys. **13**, 300 (2017).

[8] C. Zhang, S. Fukami, H. Sato, F. Matsukura, and H. Ohno, Spin-orbit torque induced magnetization switching in

nano-scale Ta/CoFeB/MgO, Appl. Phys. Lett. **107**, 012401 (2015).

[9] N. Nagaosa, J. Sinova, S. Onoda, A. H. MacDonald, and N. P. Ong, Anomalous Hall effect, Rev. Mod. Phys. **82**, 1539 (2010).

[10] B. F. Miao, S. Y. Huang, D. Qu, and C. L. Chien, Inverse Spin Hall Effect in a Ferromagnetic Metal, Phys. Rev. Lett. **111**, 066602 (2013).

[11] T. Seki, K. Uchida, T. Kikkawa, Z. Qiu, E. Saitoh, and K. Takanashi, Observation of inverse spin Hall effect in ferromagnetic FePt alloys using spin Seebeck effect, Appl. Phys. Lett. **107**, 092401 (2015).

[12] A. Tsukahara, Y. Ando, Y. Kitamura, H. Emoto, E. Shikoh, M. P. Delmo, T. Shinjo, and M. Shiraishi, Self-induced inverse spin Hall effect in permalloy at room temperature, Phys. Rev. B **89**, 235317 (2014).

[13] M. Wahler, N. Homonnay, T. Richter, A. Muller, C. Eisenschmidt, B. Fuhrmann, and G. Schmidt, Inverse spin Hall effect in a complex ferromagnetic oxide heterostructure, Sci. Rep. **6**, 28727 (2016).

[14] H. L. Wang, C. H. Du, P. C. Hammel, and F. Y. Yang, Spin current and inverse spin Hall effect in ferromagnetic metals probed by $Y_3Fe_5O_{12}$-based spin pumping, Appl. Phys. Lett. **104**, 202405 (2014).

[15] H. Wu, C. H. Wan, Z. H. Yuan, X. Zhang, J. Jiang, Q. T. Zhang, Z. C. Wen, and X. F. Han, Observation of pure inverse spin Hall effect in ferromagnetic metals via ferromagnetic/antiferromagnetic exchange-bias structures, Phys. Rev. B **92**, 054404 (2015).

[16] C. Qin, S. Chen, Y. Cai, F. Kandaz, and Y. Ji, Nonlocal electrical detection of spin accumulation generated by anomalous Hall effect in mesoscopic $Ni_{81}Fe_{19}$ films, Phys. Rev. B **96**, 134418 (2017).

[17] K. S. Das, W. Y. Schoemaker, B. J. van Wees, and I. J. Vera-Marun, Spin injection and detection via the anomalous spin Hall effect of a ferromagnetic metal, Phys. Rev. B **96**, 220408 (2017).

[18] D. C. Ralph and R. A. Buhrman, Circuits and devices based on spin hall effect to apply a spin transfer torque with a component perpendicular to the plane of magnetic layers, U.S. Patent No. 9,691,458 (Oct. 20, 2014).

[19] T. Taniguchi, J. Grollier, and M. D. Stiles, Spin-Transfer Torques Generated by the Anomalous Hall Effect and Anisotropic Magnetoresistance, Phys. Rev. Applied **3**, 044001 (2015).

[20] The Hf spacer in our sample serves to decouple the magnetic layers without inducing a separate spin Hall torque or shunting a significant amount of the applied current away from the magnetic layers. The spin Hall torque ratio for our sputtered Hf is on the order of or less than 0.01, based on repeated control measurements employing several experimental techniques with both in-plane and perpendicularly magnetized samples [21–24]. This is in contrast with measurements elsewhere that suggest larger values for the spin torque ratio of Hf (e.g., Refs. [25–27]).

[21] C.-F. Pai, M.-H. Nguyen, C. Belvin, L. H. Vilela-Leão, D. C. Ralph, and R. A. Buhrman, Enhancement of perpendicular magnetic anisotropy and transmission of spin-Hall-effect-induced spin currents by a Hf spacer layer in W/Hf/CoFeB/MgO layer structures, Appl. Phys. Lett. **104**, 082407 (2014).

[22] M.-H. Nguyen, C.-F. Pai, K. X. Nguyen, D. A. Muller, D. C. Ralph, and R. A. Buhrman, Enhancement of the anti-damping spin torque efficacy of platinum by interface modification, Appl. Phys. Lett. **106**, 222402 (2015).

[23] Y. Ou, C. F. Pai, S. Shi, D. C. Ralph, and R. A. Buhrman, Origin of fieldlike spin-orbit torques in heavy metal/ferromagnet/oxide thin film heterostructures, Phys. Rev. B **94**, 140414(R) (2016).

[24] N. Reynolds, P. Jadaun, J. T. Heron, C. L. Jermain, J. Gibbons, R. Collette, R. A. Buhrman, D. G. Schlom, and D. C. Ralph, Spin Hall torques generated by rare-earth thin films, Phys. Rev. B **95**, 064412 (2017).

[25] J. Liu, T. Ohkubo, S. Mitani, K. Hono, and M. Hayashi, Correlation between the spin Hall angle and the structural phases of early 5*d* transition metals, Appl. Phys. Lett. **107**, 232408 (2015).

[26] R. Ramaswamy, X. Qiu, T. Dutta, S. D. Pollard, and H. Yang, Hf thickness dependence of spin-orbit torques in Hf/CoFeB/MgO heterostructures, Appl. Phys. Lett. **108**, 202406 (2016).

[27] M. Akyol, W. Jiang, G. Yu, Y. Fan, M. Gunes, A. Ekicibil, P. K. Amiri, and K. L. Wang, Effect of heavy metal layer thickness on spin-orbit torque and current-induced switching in Hf|CoFeB|MgO structures, Appl. Phys. Lett. **109**, 022403 (2016).

[28] S. Honda, M. Nawate, M. Ohkoshi, and T. Kusuda, Hall Effect and Magnetic Properties in GdFe and CoCr Sputtered Films, J. Appl. Phys. **57**, 3204 (1985).

[29] U. H. Pi, K. W. Kim, J. Y. Bae, S. C. Lee, Y. J. Cho, K. S. Kim, and S. Seo, Tilting of the spin orientation induced by Rashba effect in ferromagnetic metal layer, Appl. Phys. Lett. **97**, 162507 (2010).

[30] J. Kim, J. Sinha, M. Hayashi, M. Yamanouchi, S. Fukami, T. Suzuki, S. Mitani, and H. Ohno, Layer thickness dependence of the current-induced effective field vector in Ta|CoFeB|MgO, Nat. Mater. **12**, 240 (2013).

[31] C. O. Avci, K. Garello, M. Gabureac, A. Ghosh, A. Fuhrer, S. F. Alvarado, and P. Gambardella, Interplay of S-O torque and thermoelectric effects in ferromagnet/normal-metal bilayers, Phys. Rev. B **90**, 224427 (2014).

[32] M. Hayashi, J. Kim, M. Yamanouchi, and Hideo Ohno, Quantitative characterization of the S-O torque using harmonic Hall voltage measurements, Phys. Rev. B **89**, 144425 (2014).

[33] L. Berger, Application of the side-jump model to the Hall effect and Nernst effect in ferromagnets, Phys. Rev. B **5**, 1862 (1972).

[34] T. Miyasato, N. Abe, T. Fujii, A. Asamitsu, S. Onoda, Y. Onose, N. Nagaosa, and Y. Tokura, Crossover Behavior of the Anomalous Hall Effect and Anomalous Nernst Effect in Itinerant Ferromagnets, Phys. Rev. Lett. **99**, 086602 (2007).

[35] K. Uchida, H. Adachi, T. Ota, H. Nakayama, S. Maekawa, and E. Saitoh, Observation of longitudinal spin-Seebeck effect in magnetic insulators, Appl. Phys. Lett. **97**, 172505 (2010).

[36] See Supplemental Material at http://link.aps.org/supplemental/10.1103/PhysRevApplied.9.064033 for further discussion of possible artifacts and parasitic signals

due to coupling between the two magnetic layers, the anomalous Nernst effect, and Oersted-generated torques, and how such signals may be accounted for, as well as a derivation of our second-harmonic Hall model for anomalous Hall spin currents and numerical values obtained from our fittings, a discussion of our first harmonic Hall signal fitting procedures, and a measurement of the $Fe_{95}Gd_5$ electrical anomalous Hall effect.

[37] Reference [19] also discusses a second torque mechanism that can arise from anisotropic magnetoresistance in the source layer. This other effect should be zero in our sample because the source-layer magnetization is in plane.

[38] A. M. Humphries, T. Wang, E. R. J. Edwards, S. R. Allen, J. M. Shaw, H. T. Nembach, J. Q. Xiao, T. J. Silva, and X. Fan, Observation of spin-orbit effects with spin rotation symmetry, Nat. Commun. **8**, 911 (2017).

[39] A. Bose, D. D. Lam, S. Bhuktare, S. Dutta, H. Singh, S. Miwa, and A. A. Tulapurkar, Observation of anomalous spin-torque generated by a ferromagnet, arXiv:1706.07245.

[40] See http://ralphgroup.lassp.cornell.edu/index.html.